Heritage Science

RESEARCH

Open Access

Analysis of the biocorrosion community from ancient wooden constructions at Tianluoshan (7000–6300 cal BP), Zhejiang Province, China

Biao Wang[1], Chengshuai Zhu[1], Bowen Wang[1], Bingjian Zhang[1] and Yulan Hu[1*]

Abstract

Ancient wooden constructions, also known as wooden cultural relics, refers to ancient wood that has been modified or crafted by human activities. To ensure its preservation, it is crucial to gain further understanding of the decomposition mechanisms affecting archaeological wood. In this study, we investigated the microbiome diversity and cellulose decomposition processes in a 6300-year-old ancient wooden construction at the Tianluoshan site (7000–6300 cal BP) in Zhejiang Province, China. High-throughput sequencing (HTS) was employed to analyze the metagenomic functions, specifically focusing on the microbial communities' cellulose-degrading pathways using bioinformatic approaches. The findings revealed that the excavation of archaeological wood significantly altered the environment, leading to an accelerated deterioration process. This degradation was primarily influenced by carbohydrate metabolism and xenobiotic biodegradation and metabolism pathways within the complex ecosystem consisting of bacteria, archaea, fungi, microfauna, plants, and algae. Proteobacteria, actinobacteria, ascomycota, and basidiomycota were identified as the main sources of bacterial cellulose-degrading enzymes. The results obtained from this evaluation will provide valuable insights for the development of targeted conservation strategies and prioritization of preservation efforts for the ancient wooden constructions found in different regions of the Tianluoshan site.

Keywords Cultural heritage, Conservation, Archaeological wood, Wood biodeterioration, Tianluoshan site

*Correspondence:
Yulan Hu
10507010@zju.edu.cn; hu_yulan@zju.edu.cn
Full list of author information is available at the end of the article

Graphical Abstract

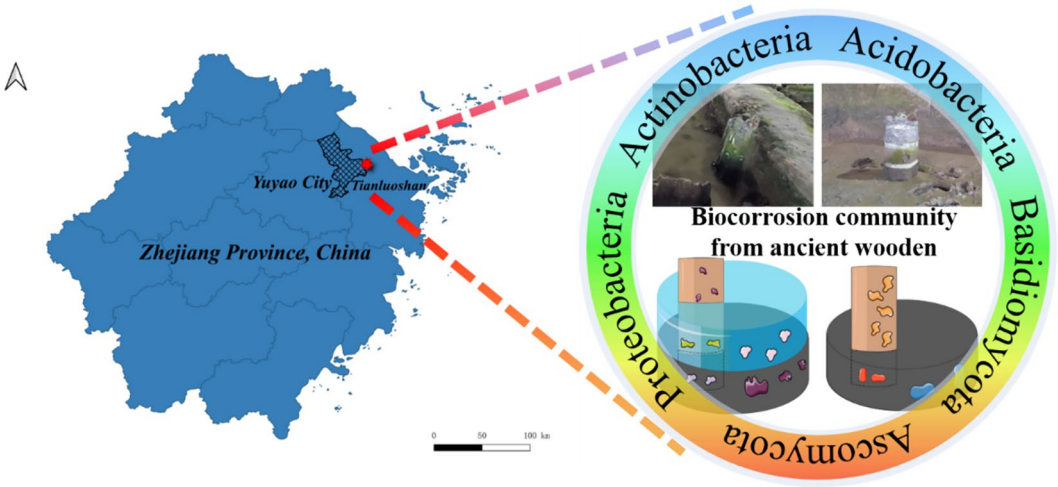

Introduction

The Tianluoshan site (7000–5800 cal BP) is located in Yuyao City, Zhejiang Province, China, and is approximately 30,000 square meters (Fig. 1) [1]. It was an important site of the Hemudu Culture [2]. During the excavations conducted from 2004 to 2007, a plethora of well-preserved archaeological materials were unearthed at the site [3]. These included wooden posts and boat paddles, as well as a variety of wooden and bone tools [4, 5]. The discovery also yielded characteristic pottery vessels and ground-stone axes [6]. Additionally, remains of animals and fish were found, indicating the presence of a diverse range of fauna in the area [7–9]. Furthermore, there were remarkably well-preserved plant remains, providing valuable insights into the local vegetation and subsistence practices of the ancient inhabitants [10, 11]. To date, eight cultural levels were excavated, and in the lower part of the site below layer 6, the artifacts are sealed in a waterlogged and anaerobic environment that results in exceptional preservation of the organic material [12].

Fig. 1 Map of the Tianluoshan site in China (121°23′E, 30°01′N)

Archaeological wood forms a large part of Chinese cultural heritage, as it has been used substantially throughout history for the construction of buildings, tools and means of transportation [13, 14]. As archaeological wood is more susceptible to erosion by natural disasters, in comparison to other cultural artifacts, archaeological wood that surpasses a span of 5000 years is exceedingly scarce [15, 16].

In past archaeological research, scholars primarily dedicated their efforts to investigating and analyzing the degradation processes of waterlogged archaeological wood recovered from marine environments [17–20]. However, the unearthed artifacts from Tianluoshan do not fall within the classification of waterlogged wood. Within the same wood, three distinct environments can be identified: exposure to air, submersion in water and burial underground. All wooden artifacts coexist within a semi-dry and semi-wet environment, presenting formidable challenges for their preservation.

In 2023, the Cultural Heritage Conservation Materials Laboratory at Zhejiang University conducted on-site puncture experiments on the ancient wooden constructions from the Tianluoshan Site. The findings revealed a significant level of decomposition in numerous ancient wooden constructions. In order to protect these remains, an understanding of the deterioration processes of wood

are essential to ensure successful management of this unique resource. Numerous studies have consistently highlighted microorganisms as one of the primary factors contributing to the degradation of cultural relics [21–23].

Carole Keepax used Scanning Electron Microscope (SEM) to observe iron-containing wooden cultural relics and found traces of fungi in the wooden samples among 32 specimens [24]. Anna Sandak use near infrared spectroscopy as a tool for archaeological wood characterization [25]. Anne Marie Eriksen utilized Fourier Transform Infrared Spectrometer (FTIR) to demonstrate that waterlogged wood loses cellulose under the erosion of Teredo navalis [26]. Daniel S and Alisa Kazarina use High throughput sequencing (HTS) to assess microbial contamination [27, 28]. In our laboratory, we have employed high-throughput sequencing techniques to investigate the intricate mechanisms behind the decay of various cultural artifacts, including grotto statues and silk objects [29–32]. However, it is important to note that existing research indicates that a singular high-throughput sequencing method alone is insufficient to fully elucidate the complex processes involved in the deterioration of cultural relics.The goal of this study was to analyze the mechanism of wood component decay through methods: SEM, Energy Dispersive Spectrometer (EDS), FTIR, X-ray diffraction (XRD) and HTS, and identify microbial communities in ancient wooden constructions at Tianluoshan (7000–6300 cal BP).

Materials and methods

Archaeological sites and morphological analysis of ancient wooden constructions

In May 2023, our laboratory undertook a comprehensive evaluation to assess the degree of decay in the ancient wooden constructions excavated from the Tianluoshan site. The Tianluoshan Site is divided into 20 regions (Figure S1). By carefully selecting representative samples from each region, we sought to gain insights into the overall condition and deterioration patterns observed among the ancient wooden constructions. To ensure the preservation and safeguarding of ancient cultural relics, our study employed self-made and enhanced pilo nail tools for conducting puncture experiments. The tool design comprised a 1 mm thick needle coupled with an adjustable pressure device. By utilizing a consistent force of 20 N, we conducted puncture experiments on ancient wooden constructions. The depth of puncture served as an indicator to estimate the degree of decay in these cultural relics (Figure S2). In our academic study, we have established a criterion to determine the decay level of ancient wooden constructions based on puncture depth. Specifically, when the puncture depth is found to be less than 10 mm, we conclude that the ancient wooden construction is experiencing mild decay. Conversely, if the puncture depth exceeds 10 mm, we consider the ancient wooden constructions to have undergone severe decay. We have conducted statistical analysis on the puncture depths of lightly decayed ancient wooden constructions across various preservation environments [33, 34].

We selected two samples for analysis, namely Sample A and Sample B (Fig. 2). Sample A was chosen to observe the effects of different environments on wooden constructions. Specifically, in Sample A, the upper end was exposed to air, the middle part was immersed in water, and the lower end was buried in soil. On the other hand, Sample B was designed to examine the impact of air exposure and soil burial without the influence of water immersion. In Sample B, only the upper end was exposed to air, while the lower end was buried in soil. (A1: Sample A is positioned at the uppermost level, exposed to air; A2: Sample A is situated on the surface of water; A3: Sample A is completely immersed in water; A4: Sample A is located on the surface layer of underwater soil; B1: Sample B1 is positioned at the highest point, exposed to air; It's worth noting that sample B1 shows signs of charring, indicating it may have been subjected to a fire before being buried in the soil; B2: Sample B is positioned in the middle layer of air; B3: Sample B is located in the shallow soil layer.) Afterward, we collected samples of water (W1) and soil (S1) from the vicinity of Sample A, as well as soil samples (S2) near Sample B.

Characterization of the ancient wooden constructions

An Hitachi SU8010 field emission scanning electron microscope (SEM) and X-ray energy spectrum detector (EDS) were used to investigate and analyze the microstructure of the wooden interface. Fourier transform infrared (FTIR) spectra were obtained using a Thermo Scientific Nicolet iS10 spectrometer in the range of 400–4000 cm^{-1} (with a 4 cm^{-1} resolution and 32 scans). The physical phase of the samples was analyzed using a Rigaku D/ MAX 2550/PC diffractometer. The test parameters were as follows: Cu Kα radiation at 250 kV, electron beam current of 40 mA, step scan method with a step size of 0.02°2θ and a scan range of 5–90°. We performed mineral phase analysis using the joint committee on powder diffraction standards (JCPDS) powder diffraction card and made a semi-quantitative component analysis of the phase in the XRD spectrum using the reference intensity ratio method in Jade analysis software.

DNA extraction and amplicon sequencing

The samples were immediately packed in sterilized centrifuge tubes and then transferred to the laboratory at low temperature for subsequent analysis. Microbial DNA extraction was carried out with modified CTAB

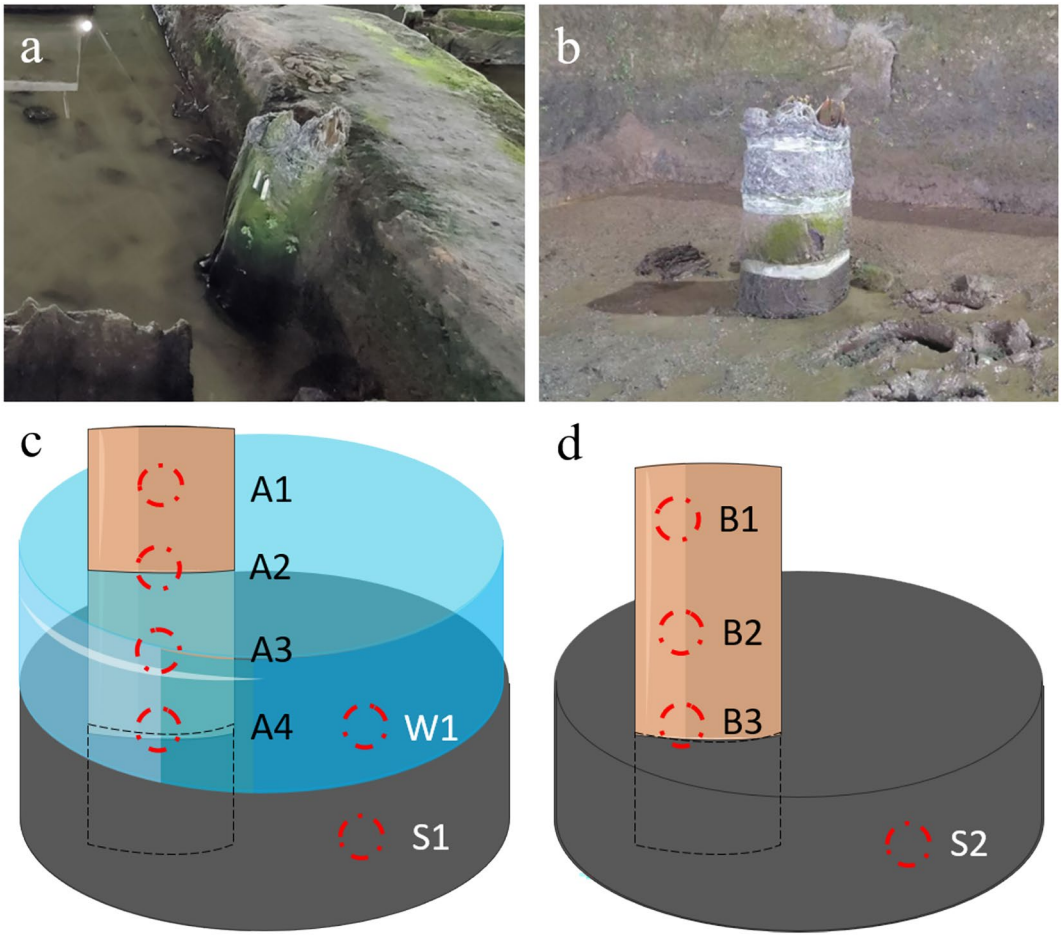

Fig. 2 Sampling point location

method (Nobleryder, China) according to the manufacturer's protocols. The 16S V3-V4 region ribosomal DNA (rDNA), internal transcribed spacer (ITS) and ITS2 region were amplified by PCR (95 °C for 5 min, followed by 30 cycles at 95 °C for 1 min, 60 °C for 1 min, and 72 °C for 1 min and a final extension at 72 °C for 7 min) with the following primers: 341F (CCT AYG GGR BGC ASC AG) and 806R (GGA CTA CNN GGG TAT CTA AT) for 16S, ITS3-2024F (GCA TCG ATG AAG AAC GCA GC) and ITS4-2409R (TCC TCC GCT TAT TGA TAT GC) for ITS. Amplicon library construction was carried out with NEB Next Ultra DNA Library Prep Kit Catalog #E7370L (Illumina, San Diego, CA, USA). Amplicons were then extracted from 2 wt.% agarose gels (Biowest, Spain) and purified with the Universal DNA Gel Purification Kit Catalog #DP214 (TianGen, China) according to the manufacturer's instructions. Throughout the DNA extraction process, ultrapure water, instead of a sample solution, was used to exclude the possibility of false-positive PCR results as a negative control. Purified amplicons were pooled in equimolar concentrations and paired end sequenced (PE250) on an Illumina platform according to the recommended protocols. (Illumina, San Diego, CA, USA) [29, 30, 32].

Taxonomic and functional analysis

The DADA2 in QIIME2 was utilized to perform a complete pipeline to turn raw paired-end fastq sequencing files into high-quality, barcode-free, merged, denoised, chimera-free, inferred sample sequences and then output operational taxonomic unit (OTU). The alpha diversity indices, Shannon, Chao1, Simpson, Faith's Phylogenetic Diversity (Faith PD) index were calculated in QIIME2. The number of sequences was rarefied to a minimum sequencing depth in both 16S and ITS OTU table to minimize the effects of sequencing depth on other analyses. OTU rarefaction curve was plotted in the R project ggplot2 package. The representative OTU sequences were classified into organisms based on Greengenes database (version 13_8) for 16S or UNITE database (version 8.2) for ITS. Top 10 phyla and genera was visualized in R

with ggplot2 and ggalluvial. Additionally, the association between microbial communities and environmental factors is also documented [29, 30, 32].

Results and discussion

Ancient wooden constructions field data

Ancient wooden constructions buried in soil exhibit good preservation, while wooden constructions submerged underwater experience accelerated decay (Fig. 3). The decay level of wooden constructions exposed to air is the most severe. The majority of wooden constructions exhibit varying degrees of decay. Therefore, it is necessary to investigate the mechanisms of decay. The puncture depths and humidity levels for samples A1, A2, and A3 were as follows: A1 had a puncture depth of 5 mm and humidity of 19%, A2 had a puncture depth of 2 mm and humidity of 41%, and A3 had a puncture depth of 1 mm and humidity of 49%. For samples B1, B2, and B3, the puncture depths and humidity levels were as follows: B1 had a puncture depth of 3 mm and humidity of 45%, B2 had a puncture depth of 5 mm and humidity of 44%, and B3 had a puncture depth of 2 mm and humidity of 58%.

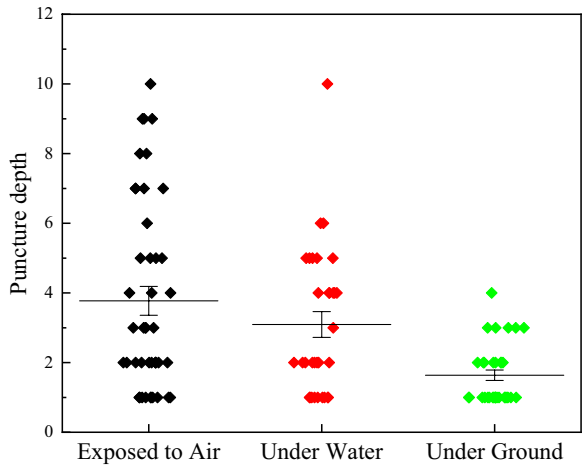

Fig. 3 The degree of decay of ancient wooden constructions at different locations

Analysis of SEM and EDS

In order to investigate the deterioration mechanism of ancient wooden constructions at Tianluoshan, photographs were captured of samples of these components under a scanning electron microscope, with magnification set at 1000 times.

The analysis of reveals the following observations about the different samples (Fig. 4). Sample A1 exhibits a significantly high degree of decay, likely due to prolonged exposure to air. Sample A2 is relatively well-preserved, possibly because it has been situated in a semi-dry and semi-wet environment, resulting in clearer fiber structures. In samples A1 and A2, microorganisms causing erosion on the wood can be clearly observed at a magnification of 10,000× (Figure S3). Sample A3, which was soaked in water for an extended period, shows signs of severe decay. The absorption and expansion of water

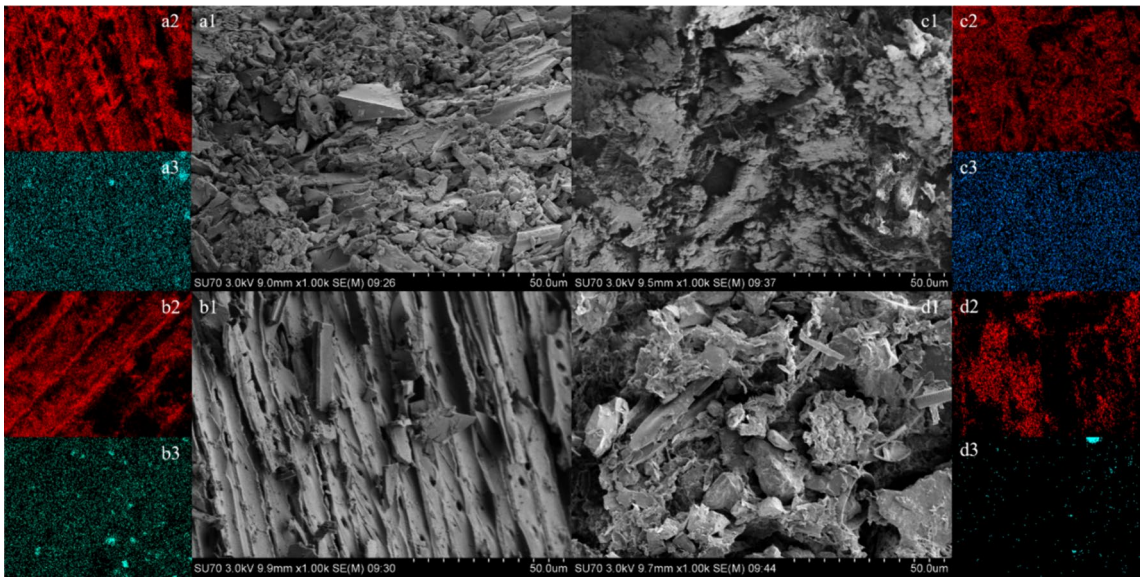

Fig. 4 a1, b1, c1, and d1 represent scanning electron microscopy images of samples A1, A2, A3, and A4, respectively. a2, b2, c2, and d2 correspond to the EDS results of carbon elements of samples A1, A2, A3, and A4, respectively. a3, b3, c3, and d3 indicate EDS results of sulfur elements of samples A1, A2, A3, and A4, respectively

have caused cell wall rupture, leading to an overall rotten appearance. Similar to Sample A3, Sample A4 is located in muddy conditions below the water surface. The long-term exposure to a humid environment causes the wooden constructions to absorb water and expand, resulting in significant decay. However, due to the protective nature of the soil, some intact fibers can still be observed in Sample A4 compared to A3.

EDS can scan the elemental proportions per unit area. Sulfur is a primary component of microbial metabolism, while carbon is a primary component of wood. The ratio of sulfur to carbon can be used to understand the abundance of sulfur-producing microbial populations. Microbial metabolism of sulfur typically exists in the form of SO_4^{2-}, and these acids contribute to the degradation of wood, which is one of the reasons for wood decay. The EDS analysis of carbon and sulfur elements reveals the following information: In terms of the proportion of sulfur element relative to carbon element, the samples can be arranged in descending order: sample A1 > sample A4 > sample A2 > sample A3. The results from EDS indicate that wood retains more sulfur when buried in soil (sample A4) and exposed to air (sample A1), while less sulfur is present in samples submerged in water (sample A2 and sample A3). The increased sulfur content in wood exposed to air is expected because the oxidation of sulfur to sulfate ions requires oxygen. In water and soil, sulfate-reducing bacteria oxidize low-valent sulfur species to sulfates under low-oxygen conditions. Sulfates in soil are deposited continuously, while those in water dissolve and eventually disperse into the water. Ultimately, wooden cultural relics that have been submerged in water for extended periods exhibit lower sulfur content (Fig. 5).

Similar to sample A, the SEM (Scanning Electron Microscopy) analysis of sample B (Fig. 4) yielded comparable results. The surface of sample B1 appeared relatively solid, indicating limited decay. This can be attributed to traces of combustion and carbonization, which effectively protected the sample from excessive deterioration. Sample B2, despite exposure to air, maintained a certain level of humidity and did not absorb water significantly. As a result, the morphology of sample B2 remained relatively intact. Sample B3, being buried in the soil for an extended period, absorbed moisture from the soil layer. This absorption led to expansion and subsequent decay, resulting in a more deteriorated appearance.

The EDS analysis of carbon and sulfur elements reveals the following information:

In terms of the proportion of sulfur element relative to carbon element, the samples can be arranged in descending order: for sample B, the order is sample B3 > sample B2 > sample B1. Upon observing sample B1, it was noted

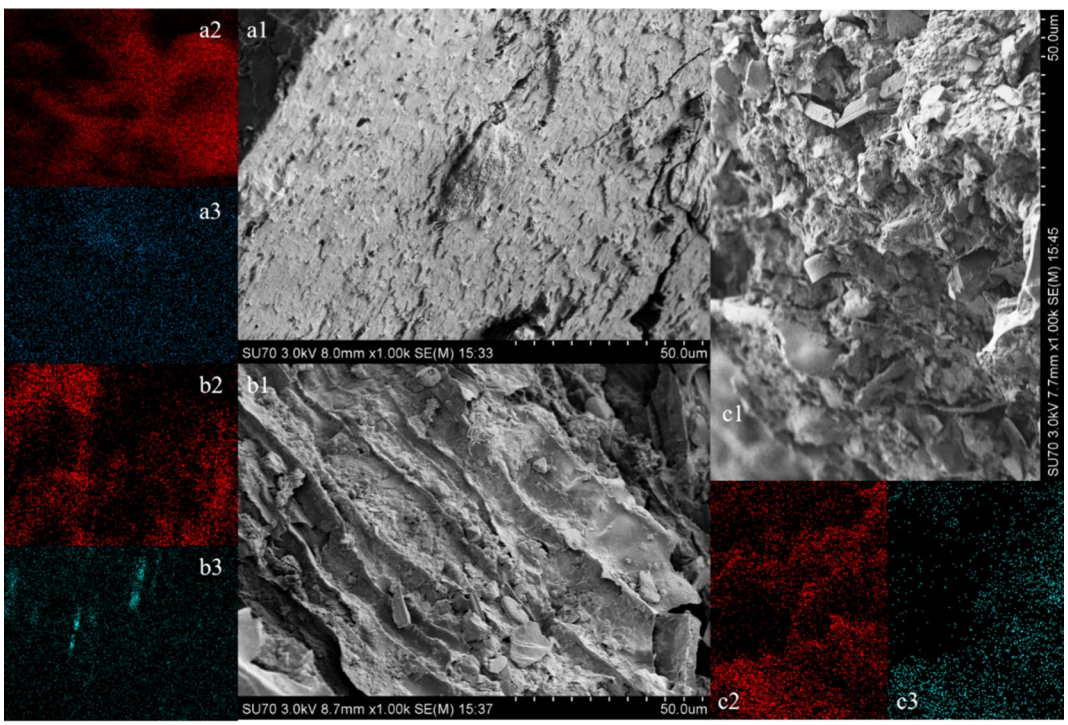

Fig. 5 a1, b1, and c1 represent SEM electron microscopy photos of samples B1, B2, and B3, respectively. a2, b2, and c2 correspond to EDS results of carbon elements in samples B1, B2, and B3, respectively.. a3, b3, and c3 indicate EDS results of sulfur elements in samples B1, B2, and B3, respectively

that its position exhibited a charred appearance, possibly due to a fire or other burning incident. This observation was confirmed by SEM images (Figure S4). Due to a similar "charred" treatment, the relative sulfur content in sample B1 is relatively low. This treatment likely reduces the presence of sulfur metabolizing microorganisms. On the other hand, samples B3 exhibit relatively high proportions of sulfur element. This suggests that samples exposed to air or buried in soil are more likely to attract sulfur metabolizing microorganisms.

Analysis of FTIR and XRD

Through analysis of the SEM images, it has been identified that the decay of ancient wooden constructions at Tianluoshan can be attributed to two primary factors. Firstly, water absorption and subsequent expansion occur as a result of osmotic pressure. Secondly, microbial erosion contributes to the process of decay and rotting. Through FTIR analysis, it is possible to determine the specific factors that lead to a more pronounced depletion of organic constituents in wooden constructions (Fig. 6).

The infrared spectrum analysis reveals specific absorption peaks that provide insights into the composition of the samples: The absorption peak observed at 3423 cm^{-1} corresponds to aliphatic hydroxyl and phenolic hydroxyl groups (O–H) present in lignin. The absorption peak at 2920 cm^{-1} is attributed to methoxy or fatty methyl or methylene groups (C-H) within lignin. The absorption peak located at 1594 cm^{-1} represents the benzene ring structure (C=C) of lignin. A characteristic peak at 1043 cm^{-1} is indicative of cellulose and hemicellulose components (C–O–C) [34–36]. These spectral features aid in identifying and characterizing the presence of different organic functional groups in the analyzed samples, shedding light on the composition of the lignocellulosic materials.

C-H and O–H functional groups are commonly found in lignin, cellulose, and hemicellulose, which are the main components of wood materials. Therefore, we mainly focus on discussing the C–O–C and C=C functional groups. A semi-quantitative analysis of the areas under the four FTIR characteristic peaks indicates that the areas for the C–O–C characteristic peaks in sample A1 is 31% and sample B1 is 28% (Figure S5). The proportion of characteristic peak area of C–O–C represents the content of cellulose and hemicellulose. Samples A2, A3, A4, B2, and B3 have C–O–C characteristic peak area proportions ranging from 35 to 43%. Therefore, it can be inferred that the cellulose and hemicellulose in samples A1 and B1 has undergone more erosion. The most representative functional group of lignin is C=C. The characteristic peak area of C=C in samples A1 and A4 is higher than that in samples A2 and A4, indicating that wood exposed to water is more prone to lignin loss. Sample B1 has a higher abundance of C=C functional groups. This is because sample B1 has been exposed to a fire incident, resulting in the loss of more easily combustible cellulose and the retention of more lignin structures. Sample B2 is in a relatively dry environment, while sample B3 is in moist soil, leading to a greater loss of lignin in sample B3.

This finding indicates that the preservation of wooden artifacts in water or soil is more effective than when exposed to air. Water or soil creates a closed environment, reducing the influx of oxygen and inhibiting the growth of microorganisms, thus minimizing the degradation of organic components in wooden constructions. Conversely, when wooden constructions are exposed to air, a favorable environment for microbial proliferation is created, resulting in a decline in organic content and subsequent decay of the wooden constructions. In order

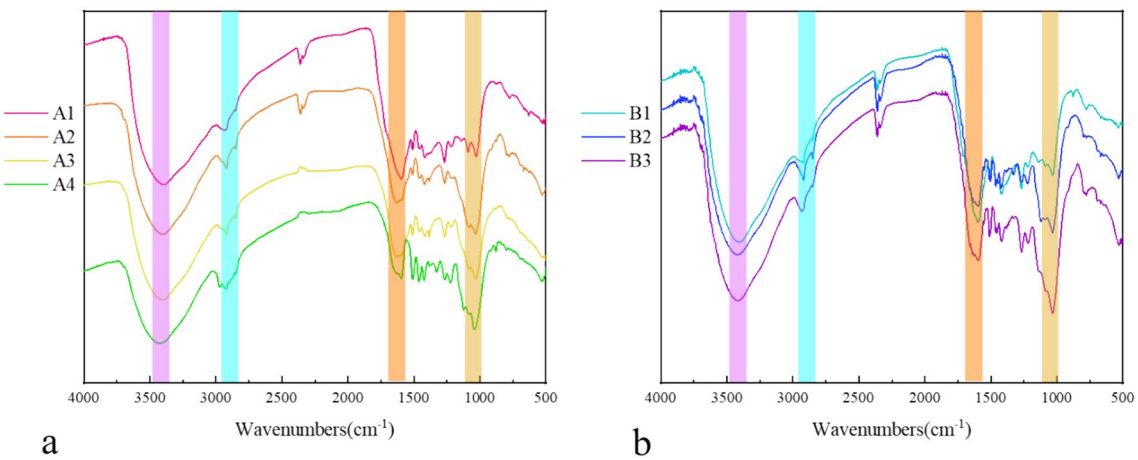

Fig. 6 **A** presents the FTIR of sample A, **B** displays the FTIR of sample B

to identify the soil composition, FTIR analysis was conducted on samples S1 and S2 as well.

The analysis of the infrared spectra reveals several absorption peaks and their corresponding assignments (Fig. 7): The 3622 cm^{-1} and 3422 cm^{-1} peaks correspond to the OH vibration absorption peak of the silicate crystal layer. At 2922 cm^{-1}, the absorption peak represents the stretching vibration of -CH bonds. The absorption peak at 1629 cm^{-1} may indicate the presence of N–O or C=O bonds within organic matter. A strong absorption peak at 1035 cm^{-1} can be attributed to Si–O–Si vibrations. Weak absorption peaks at 794 cm^{-1} and 693 cm^{-1} are associated with Si–O vibrations. At 524 cm^{-1}, an absorption peak indicates Al-O vibrations and -OH absorption peak. Based on FTIR analysis, it is hypothesized that the soil contains silicon dioxide, quartz, and chlorite as components. The specific components need to be determined through XRD analysis. Through XRD analysis, it can be concluded that the following observations were made: At $2\theta = 26.7$, an X-ray diffraction peak corresponding to SiO_2 was observed. At $2\theta = 8.9$, an X-ray diffraction peak attributed to muscovite was observed. At $2\theta = 6.3$, 12.6, and 60.0, X-ray diffraction peaks indicating the presence of clinochlore were observed. At $2\theta = 22.1$, an X-ray diffraction peak associated with cristobalite was observed. At $2\theta = 20.9$ and 50.2, X-ray diffraction peaks representing microcline were observed. By analyzing the XRD data combined with FTIR, it can be concluded that samples S1 and S2 have a similar composition. Both samples primarily consist of SiO_2 (silicon dioxide), muscovite, clinochlore, cristobalite, and microcline [37–40]. These components are identified based on their characteristic diffraction patterns and infrared absorption bands observed in the analysis. Silicon dioxide (SiO_2) is a major component of many rocks and minerals, providing silicon as an essential nutrient for certain microorganisms. Muscovite is a common mica mineral that contains potassium, which is utilized by various microbes for metabolic processes. Clinochlore is a type of chlorite mineral that offers magnesium and iron, important elements needed by microorganisms. Cristobalite, another form of silica, can provide a source of silicon for microbial utilization. Microcline, a feldspar mineral, contains potassium, which serves as a vital nutrient for microbial growth. These minerals play a significant role in providing essential elements necessary for the development and sustenance of microbial communities.

Based on semi-quantitative analysis of samples S1 and S2 (Figure S6), it was found that the proportion of cristobalite in sample S1 is less than 0.1%, while in sample S2, it is 14.9%. The proportion of clinochlore in sample S1 is 29.2%, whereas in sample S2, it is 10.7%. Additionally, there is a decrease in the proportion of muscovite in sample S2. The microbial community in soil is closely related to the physicochemical properties of the soil. Environmental differences lead to variations in the microbial communities that thrive. Samples S1 and S2 exhibit significant differences in the content of silicate minerals and mica minerals. This provides a basis for detecting different microorganisms in soil samples in subsequent high-throughput sequencing.

Taxonomic analysis and diversity of microbial community as determined by HTS.

After quality filtering, a total of 15,671 and 1441 OTUs was obtained from the 16S and ITS sequences, respectively. We visualized the dominant (top 10) prokaryotic (Fig. 8A1) and eukaryotic (Fig. 8B1) phyla among all samples. The dominant (top 10) prokaryotic (Fig. 8A2) and

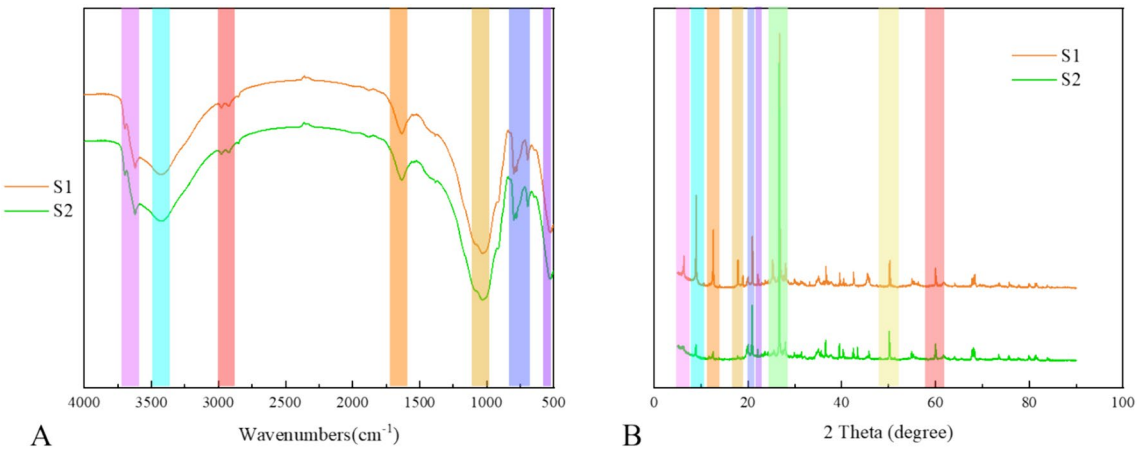

Fig. 7 The FTIR (**A**) and XRD (**B**) of sample S1 and S2

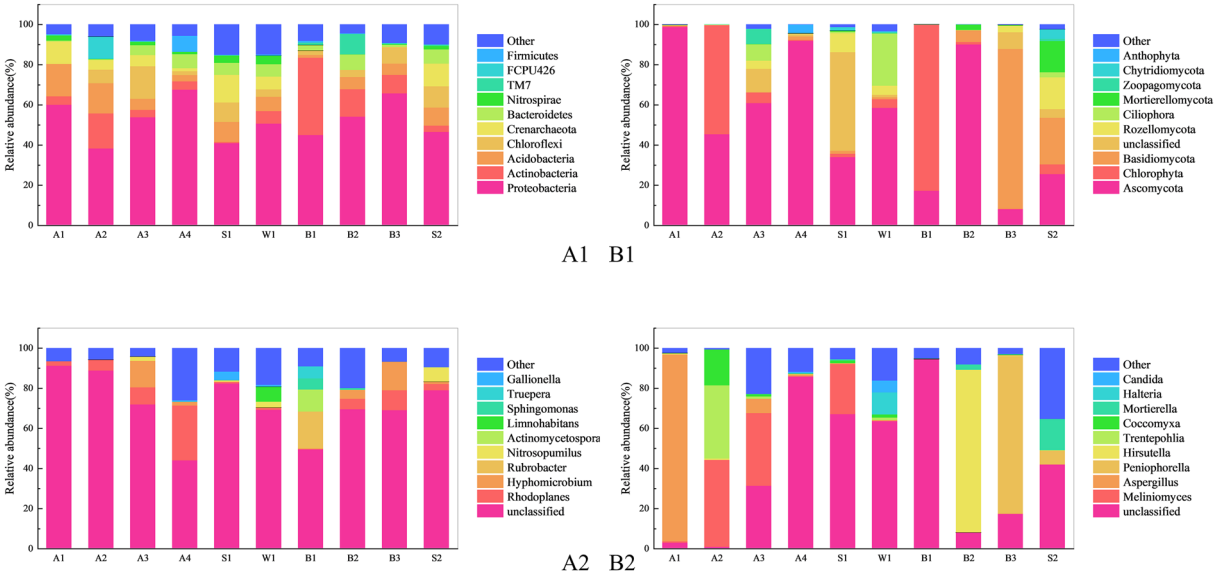

Fig. 8 Taxonomic analysis of microbial communities in the samples. The dominant prokaryotic phyla in the samples (A1) and The dominant eukaryotic phyla in the samples (B1). Taxonomic analysis of microbial communities in the samples. The dominant prokaryotic genera in the samples (A2) and The dominant eukaryotic genera in the samples (B2)

eukaryotic (Fig. 8B2) genus among all samples are also visualized.

The top 10 dominant prokaryotic phyla are proteobacteria, actinobacteria, acidobacteria, chloroflexi, crenarchaeota, bacteroidetes, nitrospirae, TM7, FCPU426, firmicutes. The top 10 dominant eukaryotic phyla are ascomycota, chlorophyta, basidiomycota, unclassified, rozellomycota, ciliophora, mortierellomycota, zoopagomycota, chytridiomycota, anthophyta. The top 10 dominant prokaryotic genu are unclassified, rhodoplanes, hyphomicrobium, rubrobacter, nitrosopumilus, actinomycetospora, limnohabitans, sphingomonas, truepera, gallionella, and other. The top 10 dominant eukaryotic genus are unclassified, meliniomyces, aspergillus, peniophorella, hirsutella, trentepohlia, coccomyxa, mortierella, halteria, candida, and other.

In the samples, the most represented phylum appeared to be proteobacteria, with a relative abundance of 50%. Proteobacteria is a common bacterial colony found on cultural relics [41, 42]. At the genus level within the phylum proteobacteria, rhodoplanes and hypomicrobium are major microbial communities. Rhodoplanes exhibit a relatively high proportion in ancient wooden constructions A, with proportions of 2.3%, 5.5%, 8.6%, and 27.4% in samples A1, A2, A3, and A4, respectively. The abundance of hypomicrobium in sample A3 is 13.2%. Hypomicrobium is worth noting in the decay process of wooden cultural relics because it can survive in both aerobic and anaerobic environments, making it ubiquitous in many locations. Both the water environment (W1) and soil environment (S1), where sample A is located, harbor diverse prokaryotic communities. These prokaryotic communities contain all the prokaryotic genus in sample A. In addition to the Proteobacteria phylum, other prokaryotes have also been detected. In the sample A1, the represented phylum are acidobacteria and crenarchaeota, with a mean relative abundance of 16.2% and 11.1%. In sample A2, actinobacteria, acidobacteria, and FCPU426 exhibited abundances of 17.4%, 15.1%, and 11.1%, respectively. In sample A3, the relative abundance of chloroflexi was observed to be relatively high, at 16.2%. In the sample A4, the represented phylum are actinobacteria and acidobacteria, with a mean relative abundance of 4.2% and 3.1%. Both Sample A1 and Sample A2 are in the air. In the sample A1, acidobacteria and crenarchaeota are the main representative phyla, possibly due to airborne microbes mainly originating from suspended particles and dust. Acidobacteria, known for their ability to degrade organic matter in the air, exhibit a higher relative abundance. As Sample A2 is often in a humid environment, it will harbor a large amount of Actinobacteria and FCPU426. The sample A3 completely submerged in water, chloroflexi exhibit a higher relative abundance. Aquatic ecosystems typically support the growth and proliferation of waterborne microbes like chloroflexi, thus showing a higher relative abundance in water-submerged samples. Sample A4 buried in soil, low concentration of oxygen may result in lower relative abundances of Actinobacteria and AcidobacteriaIn the samples B1, B2, and B3, actinobacteria emerged as the

most dominant phylum, exhibiting mean relative abundances of 38.6%, 16.2%, and 11.1%, respectively. However, notable variations in the abundance of actinobacteria were observed among the wooden samples. Additionally, it is worth mentioning that TM7 had a relatively high abundance of 10.1% in the B2 samples, which adds to the interesting findings of our study. In sample B1, the relative abundance of Actinobacteria is 38.6%, which is close to the abundance of Proteobacteria. This could be due to the relatively lower cellulose content and higher lignin content in sample B1 compared to samples B2 and B3. Lignin attracts more Actinobacteria parasitism. When wood components are exposed to air (sample B2), suitable humidity and temperature conditions make TM7 the dominant bacterial species. Sample B3 is buried in somewhat moist soil, and although Actinobacteria still dominate the community, their abundance is relatively low. This could be due to competition from other microorganisms in the soil or the influence of soil humidity on the growth of Actinobacteria.The prokaryote present in the water and soil surrounding the wooden constructions were also thoroughly identified. The abundance of prokaryote in water is relatively uniform. Moreover, in soil samples S1 and S2, a relatively high abundance of acidobacterium, chloroflexi, and crenarchaeota was observed.

Through analysis of abundance profiles at the level of the prokaryote kingdom, it is evident that the phylum proteobacteria is a ubiquitous community in all samples. However, the sample preservation environment has led to distinct microbial communities in different samples [43–45].

In sample B1, rubrobacter is found to have the highest abundance, accounting for 18.2% of the microbial community. Samples B2, B3, and S2 demonstrate distinct microbial communities, with rhodoplanes and hyphomicrobium comprising a relatively high proportion. Among these samples, rhodoplanes represents 5.2%, 9.9%, and 3.2% of the three samples, respectively, while hyphomicrobium accounts for 4.3%, 14.3%, and 1.14% of the three samples, respectively. Through the analysis of abundance profiles at the genus level of prokaryotes, it is evident that the rhodoplanes community is the dominant population in sample A. However, due to the lower moisture levels in the environment of sample B, there are dominant communities of not only rhodoplanes but also rubrobacter and hyphomicrobium.

Eukaryotic microorganisms are an important component of microbial communities. A large number of ascomycetes were detected in all samples, exhibiting mean relative abundances of 98.5%, 45.1%, 60.7%, 91.7%, 16.9%, 89.9% and 7.8%, in samples A1, A2, A3, A4, B1, B2 and B3, respectively. Ascomycota are highlighted as playing a significant role in the degradation of organic matter in wooden constructions, indicating their importance in ecological processes related to wood decay. In samples A2 and B1, chlorophyta takes precedence as the dominant community, exhibiting mean relative abundances of 60.7%, and 16.9%. Sample A2, due to its moist environment, provides favorable conditions for the growth of Chlorophyta. However, in the drier environment of sample A1, the fully submerged condition of sample A3, and the complete burial in soil of sample A4, Chlorophyta did not become the predominant microbial community in samples A1, A3, and A4. Compared to the sample B1 (Figure S4), which presents a charred surface, sample B2 is more conducive to the growth of Ascomycetes. More Ascomycetes will accumulate at the location of sample B2, resulting in a higher abundance of Ascomycetes in sample B2. Consequently, the Chlorophyta from sample B2 will enrich at the location of sample B1. In sample B3, basidiomycota emerges as the dominant community, exhibiting mean relative abundances of 79.8% [46, 47]. The damp soil and suitable organic matter create an ideal environment for the growth of Basidiomycota. Therefore, sample B3, buried in soil, becomes a more suitable choice for growth. Ciliophora is a phylum of unicellular eukaryotes that are common and have pivotal roles in aquatic environments [48]. So, a substantial presence of ciliophora (16.1%) was detected in sample W1. Sample S1, being a sludge situated underwater, exhibited the presence of numerous unclassified eukaryotes. In contrast to sample S1, which is located underwater, sample S2 is situated on land. In sample S2, a significant abundance of ascomycota, basidiomycota, rozellomycota, and mortierellomycota communities has been detected, exhibiting mean relative abundances of 25.3%, 23.3%, 15.9%, and 15.5%, respectively.

Through the analysis of abundance profiles at the level of eukaryote phyla, it is observed that both sample A and sample B exhibit a substantial population of ascomycota, which is primarily responsible for the degradation of organic matter in wooden constructions. Furthermore, our investigation revealed a significant presence of basidiomycota in sample B3, suggesting favorable conditions for its growth in the topsoil from where B3 sample was obtained. Moreover, abundant communities of chlorophyta were detected in both aquatic and soil environments, but they were scarce on the wooden structure. Consequently, it can be concluded that green algae are not the primary cause of wood decay [49–54].

In sample A1, the abundance of aspergillus is notably high, reaching 93.4%. Meliniomyces exhibits the highest abundance in sample A2, A3, and S1, with proportions of 43.4%, 36.3%, and 25.0%, respectively. The abundance of halteria in sample W1, which represents the water

environment where sample A is located, is recorded as 11.0%. Sample B2 displays the highest abundance of hirsutella at 81.1%. In sample B3, peniophorella emerges as the dominant community, with an abundance of 78.6%. Sample S2 demonstrates the highest abundance of mortierella, amounting to 15.5%. On the other hand, samples A4 and B1 do not exhibit significant eukaryotic communities. Sample A4 is located in soil, it is subjected to a relatively anaerobic environment, making it difficult for eukaryotic microorganisms to thrive. Sample B1 may have undergone a fire, as evidenced by its charred surface (Figure S4), and concurrently has a lower cellulose content, which hinders the provision of nutrients necessary for the survival of eukaryotic microorganisms.

Through the analysis of abundance profiles at the genus level of prokaryotes, it is evident that the abundance of aspergillus in sample A reaches a remarkable level of 93.4%. This finding is further supported by scanning electron microscopy, confirming that aspergillus is the primary contributor to decay in sample A (Figure S3). However, samples A2 and A3 exhibit minimal presence of aspergillus but a significant population of meliniomyces. This disparity can be attributed to the excessively moist environment, which inhibits the growth of aspergillus communities. Moreover, sample A4 demonstrates a lesser degree of decay and no dominant species at the eukaryote genus level, suggesting that water and soil can provide an anaerobic environment to some extent, thus offering protection to the wooden structure.

In contrast, sample B1 lacks any dominant species at the eukaryote genus level, indicating a scarcity of organic matter in the charred sample. Consequently, the availability of a favorable survival environment for eukaryotic organisms is limited, resulting in partial protection of the wooden structure. Conversely, sample B2 exhibits significant growth of hirsutella, a fungus that prefers parasitizing within animal bodies, thereby, limiting its impact on the wooden structure. As for sample B3, originating from the topsoil layer, the dominant community consists of peniophorella, another type of fungus with the potential to cause wood decay, necessitating appropriate treatment measures [55].

CCA/RDA analysis

In this particular analysis, the environmental factors selected for conducting the CCA analysis on samples A and B of ancient wooden constructions were the puncture depth and humidity. These factors were chosen to explore their influence on the microbial communities associated with the wooden constructions. The analysis of CCA/RDA (Canonical Correspondence Analysis/Redundancy Analysis) primarily relies on the utilization of the R language VEGAN package, along with visualization techniques using ggplot2. CCA/RDA & DCA (Detrended correspondence analysis) analysis is a sorting method that combines correspondence analysis with multiple regression analysis. Each calculation step involves regression with environmental factors, referred to as multiple direct gradient analysis. RDA is based on a linear model, while CCA is based on a unimodal model. In this report, DCA analysis will be initially performed to assess if the maximum axis value exceeds 4.0. If it surpasses 4.0, CCA will be chosen; otherwise, RDA will be applied. The purpose of this analysis is primarily to examine the relationship between microbial communities and environmental factors. It can detect connections between environmental factors, samples, and microbial communities, or identify associations between pairs, ultimately identifying significant environmental drivers that influence sample distribution.

The basic data of Fig. 9 is: the puncture depths and humidity levels for samples A1, A2, and A3 were as follows: A1 had a puncture depth of 5 mm and humidity of 19%, A2 had a puncture depth of 2 mm and humidity of 41%, and A3 had a puncture depth of 1 mm and humidity of 49%. For samples B1, B2, and B3, the puncture depths and humidity levels were as follows: B1 had a puncture depth of 3 mm and humidity of 45%, B2 had a puncture depth of 5 mm and humidity of 44%, and B3 had a puncture depth of 2 mm and humidity of 58%. Since there was insufficient data available for samples A4 and B4 to complete the RDA/CCA analysis, we have provided speculated environmental factor data. We assume that both A4 and B4 are located in a soil environment, and due to long-term immersion in water, the humidity increases to 75%. Additionally, considering the well-preserved nature of the ancient wooden constructions in the soil, we select a puncture depth of 1 mm.

Based on the RDA analysis of prokaryotes, it has been observed that prevotella, alistipes, nitrosopumilus, fusobacterium, pseudomonas, streptococcus, phenonobacterium, rhodoplanes, bacteroides, and nitrospira exhibit a preference for environments with high humidity. Based on the CCA analysis of eukaryote, it has been observed that peniophorella, penicillium, fusarium, mortierella, cladosporium, alternaria, ciliophora, phlyctochytrium, coelastrella, meripilus, nigrospora and triticum exhibit a preference for environments with high humidity. By combining the previous results of microbial sequencing, it becomes evident that rhodoplanes, peniophorella, and mortierella have a preference for thriving in environments with high humidity. Furthermore, aspergillus demonstrates a particular affinity for colonizing wooden constructions that display advanced stages of decay. This is consistent with the frequent presence of

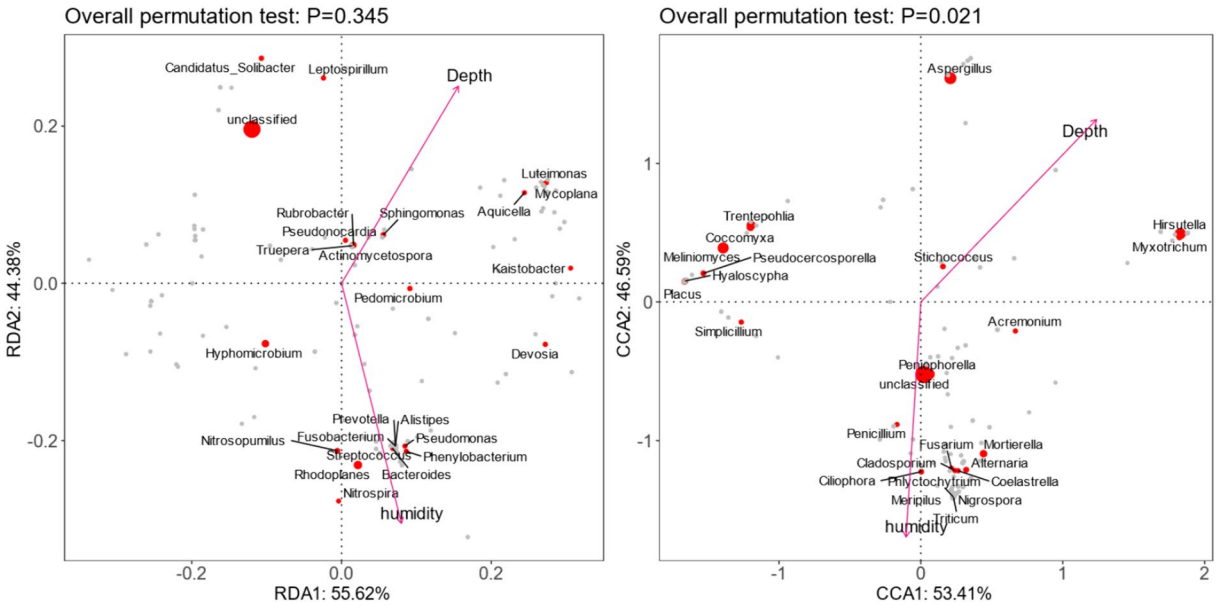

Fig. 9 RDA and CCA analysis (the left side depicts the RDA analysis conducted on prokaryote, while the right side showcases the CCA analysis performed on eukaryote)

microorganisms such as Rhodoplanes and Aspergillus in humid environments[56, 57].

Conclusion

Through the sampling and analysis of ancient wooden constructions at the Tianluoshan site, it has been determined that wood decay is primarily caused by two factors. Firstly, when wooden constructions are buried in soil or water, they tend to absorb moisture and expand due to osmotic pressure. Secondly, when wooden constructions are exposed to the air, they become vulnerable to colonization by a diverse array of microorganisms, resulting in decay. The microbial phyla predominantly associated with wood decay include proteobacteria, actinobacteria, acidobacteria, basidiomycota and ascomycota. At the genus level, key microbial taxa responsible for wood decay encompass rhodoplanes, rubrobacter, hyphomicrobium, aspergillus, melinomyces, hirsutella, and peniophorella, the genus aspergillus is particularly noteworthy. SiO_2 (silicon dioxide), muscovite, clinochlore, cristobalite, and microcline are mineral components that contribute crucial elements for microbial growth. Through the analysis of the overall microbial community, it is evident that archaeological wooden components experience less microbial erosion when buried in soil. When exposed to air, moisture and oxygen provide suitable conditions for microbial survival, leading to further deterioration of archaeological wooden components. The wooden components at the Tianluoshan site are immovable, and a new conservation strategy involves constructing a 'aquarium' on-site. This would involve adding water and removing oxygen from the water to protect the wooden components while also serving as an exhibition. In our future endeavors, we will develop preservation strategies tailored to these specific types of microorganisms, with the aim of retarding the decay process of ancient wooden constructions.

Supplementary Information

The online version contains supplementary material available at https://doi.org/10.1186/s40494-024-01304-3.

Supplementary Material 1.

Acknowledgements

Special thanks go to Junior Qin Y for proofreading this article. We are particularly grateful to the staff at the Tianluoshan Site Exhibition Hall and my colleagues (Wu Q, Chen MT, Qi MY, Fang XX, Du BB, Liu ZD, Wang X, Sun XL and Cai JQ) for their support in this study.

Author contributions

Biao Wang. wrote the main manuscript text; Biao Wang, Chengshuai Zhu and Bowen Wang: Data Curation and prepared Figs. 1, 2, 3, 4, 5. 6, 7, 8and9. Bingjian Zhang and Yulan Hu: Conceptualization, Funding Acquisition, Resources, Supervision, Writing—Review & Editing. All authors reviewed the manuscript.

Funding

This work was supported by the Scientific Research Fund of Zhejiang Cultural Heritage Conservation Science and Technology Project (Project Number: 2024008; Project Name: Wetland Conservation of Wooden Cultural Relics and Research on Display Application: A Case Study of Field Protection at Tianluoshan for Wooden Relics).

Data availability
The data that support the findings of this study are available from the corresponding author, Yulan Hu, upon reasonable request.

Declarations

Ethics approval and consent to participate
Our study did not require further ethics committee approval as it did not involve animal or human clinical trials and was not unethical.

Competing interests
We declare that we have no financial and personal relationships with other people or organizations that can inappropriately influence our work, there is no professional or other personal interest of any nature or kind in any product, service and/or company that could be construed as influencing the position presented in, or the review of, the manuscript entitled.

Author details
[1]Department of Archaeology, Cultural Heritage and Museology, Zhejiang University, Hangzhou 310028, China.

Received: 20 March 2024 Accepted: 27 May 2024
Published online: 11 June 2024

References

1. Sun G, Huang W, Zheng Y, Liu Z, Xu Z, Qu K, et al. Brief report of the excavation on a neolithic site at Tianluoshan Hill In Yuyao City, Zhejiang Province (In Chinese). Cult Relics. 2007;11:4–24, 73.
2. Minglin L, Duowen M, Longjiang M, Guoping S, Kunshu Z. Paleosalinity in the Tianluoshan site and the correlation between the Hemudu culture and its environmental background. J Geogr Sci. 2010. https://doi.org/10.1007/s11442-010-0441-1.
3. Dorian F, Ling Q, Yunfei Z, Zhao Z, et al. The domestication process and domestication rate in rice: spikelet bases from the lower Yangzte. Science. 2009;5921(323):1607–10.
4. Cameron J, Sun G. Textile production and craft specialisation at Tianluoshan in the lower Yangzi valley. Antiquity. 2022;96(389):1124–41. https://doi.org/10.15184/aqy.2022.104.
5. Yunfei Z, Guoping S, Ling Q, Chunhai L, Xiaohong W, Xugao C. Rice fields and modes of rice cultivation between 5000 and 2500 BC in east china. J Archaeol Sci. 2009;36(12):2609–16. https://doi.org/10.1016/j.jas.2009.09.026.
6. Dong J, Sun G, Wang N, Lou H, Li Q, Gu D. Analysis the neolithic Jade Jue unearthed from three sites in Zhejiang. Spectrosc Spectralanal. 2017;37(9):2905–13. https://doi.org/10.3964/j.issn.1000-0593(2017)09-2905-09.
7. Hsu K, Eda M, Kikuchi H, Sun G. Neolithic avifaunal resource utilisation in the lower Yangtze river: a case study of the Tianluoshan site. J Archaeol Sci Rep. 2021;37:102929. https://doi.org/10.1016/j.jasrep.2021.102929.
8. Nakajima T, Nakajima M, Mizuno T, Sun GP, He SP, Liu HZ. On the pharyngeal tooth remains of crucian and common carp from the Neolithic Tianluoshan Site, Zhejiang Province, China, with remarks on the relationship between freshwater fishing and rice cultivation in the neolithic age. Int J Osteoarchaeol. 2012;22(3):294–304. https://doi.org/10.1002/oa.1206.
9. Zhang Y, Sun G, Wang Y, Huang Y, Kikuchi H, Yang X. Sustainable hunting strategy of sika deer (*Cervus nippon*) in the Neolithic Lower Yangtze River Region, China. Front Earth Sci. 2022. https://doi.org/10.3389/feart.2021.812910.
10. Carey J. Unearthing the origins of agriculture. Proc Natl Acad Sci. 2023. https://doi.org/10.1073/pnas.2304407120.
11. Zheng Y, Sun G, Chen X. Characteristics of the short Rachillae of rice from archaeological sites dating to 7000 years ago. Chin Sci Bull. 2007;52(12):1654–60. https://doi.org/10.1007/s11434-007-0258-1.
12. Guo Y, Wu R, Sun G, Zheng Y, Fuller BT. Neolithic cultivation of water chestnuts (trapa l.) At tianluoshan (7000–6300 cal bp), Zhejiang Province, China. Sci Rep. 2017. https://doi.org/10.1038/s41598-017-15881-w.
13. Florian M. Scope and history of archaeological wood. Adv Chem Ser. 1990;225:3–32.
14. Walsh-Korb Z. Sustainability in heritage wood conservation: challenges and directions for future research. Forests. 2022;13(1):18. https://doi.org/10.3390/f13010018.
15. Marais BN, Brischke C, Militz H. Wood durability in terrestrial and aquatic environments - a review of biotic and abiotic influence factors. Wood Mat Sci Eng. 2022;17(2):82–105. https://doi.org/10.1080/17480272.2020.1779810.
16. Walsh-Korb Z, Avérous L. Recent developments in the conservation of materials properties of historical wood. Progr Mater Sci. 2019;102:167–221. https://doi.org/10.1016/j.pmatsci.2018.12.001.
17. Cao H, Gao X, Chen J, Xi G, Yin Y, Guo J. Changes in moisture characteristics of waterlogged archaeological wood owing to microbial degradation. Forests. 2023;14(1):9. https://doi.org/10.3390/f14010009.
18. Li Q, Cao L, Wang W, Tan H, Jin T, Wang G, et al. Analysis of the bacterial communities in the waterlogged wooden cultural relics of Thexiaobaijiao no. 1 shipwreck via high-throughput sequencing technology. Holzforschung. 2018;72(7):609–19. https://doi.org/10.1515/hf-2017-0132.
19. Liu Z, Fu T, Hu C, Shen D, Macchioni N, Sozzi L, et al. Microbial community analysis and biodeterioration of waterlogged archaeological wood from the Nanhai no. 1 shipwreck during storage. Sci Rep. 2018;8(1):7170. https://doi.org/10.1038/s41598-018-25484-8.
20. Singh AP, Kim YS, Chavan RR. Advances in understanding microbial deterioration of buried and waterlogged archaeological woods: a review. Forests. 2022;13(3):394. https://doi.org/10.3390/f13030394.
21. Bjordal CG, Naturvetenskapliga F, et al. Microbial degradation of waterlogged archaeological wood. J Cult Herit. 2012;13(3):S118–22. https://doi.org/10.1016/j.culher.2012.02.003.
22. Kim YS, Singh AP, Nilsson T. Bacteria as important degraders in waterlogged archaeological woods. Holzforschung. 1996;50(5):389–92. https://doi.org/10.1515/hfsg.1996.50.5.389.
23. Singh AP. A review of microbial decay types found in wooden objects of cultural heritage recovered from buried and waterlogged environments. J Cult Herit. 2012;13(3):S16–20. https://doi.org/10.1016/j.culher.2012.04.002.
24. Keepax C. Scanning electron microscopy of wood replaced by iron corrosion products. J Archaeol Sci. 1975;2(2):145–50. https://doi.org/10.1016/0305-4403(75)90033-3.
25. Sandak A, Sandak J, Zborowska M, Prądzyński W. Near infrared spectroscopy as a tool for archaeological wood characterization. J Archaeol Sci. 2010;37(9):2093–101. https://doi.org/10.1016/j.jas.2010.02.005.
26. Eriksen AM, Gregory D, Shashoua Y. Selective attack of waterlogged archaeological wood by the shipworm, teredo navalis and its implications for in-situ preservation. J Archaeol Sci. 2015. https://doi.org/10.1016/j.jas.2014.12.011.
27. Jones DS, Monnier G, Cooper A, Baković M, Pajović G, Borovinić N, et al. Applying high-throughput rRNA gene sequencing to assess microbial contamination of a 40-year old exposed archaeological profile. J Archaeol Sci. 2021;126:105308. https://doi.org/10.1016/j.jas.2020.105308.
28. Kazarina A, Gerhards G, Petersone-Gordina E, Kimsis J, et al. Analysis of the bacterial communities in ancient human bones and burial soil samples: tracing the impact of environmental bacteria. J Archaeol Sci. 2019;109:104989. https://doi.org/10.1016/j.jas.2019.104989.
29. Wang B, Qi M, Ma Y, Zhang B, Hu Y. Microbiome diversity and cellulose decomposition processes by microorganisms on the ancient wooden seawall of Qiantang river of Hangzhou, china. Microb Ecol. 2023;86(3):2109–19. https://doi.org/10.1007/s00248-023-02221-x.
30. Wang B, Zhu C, Hu Y, Zhang B, Wang J. Dynamics of microbial community composition during degradation of silks in burial environment. Sci Total Environ. 2023. https://doi.org/10.1016/j.scitotenv.2023.163694.
31. Zhu C, Wang B, Tang M, Wang X, et al. Analysis of the microbiomes on two cultural heritage sites. Geomicrobiol J. 2023;40(2):203–12. https://doi.org/10.1080/01490451.2022.2137604.
32. Zhu C, Wang L, Wang B, Wang B, Tang M, Wang X, et al. Application and evaluation of a new blend of biocides for biological control on cultural heritages. Int Biodeterior Biodegrad. 2023. https://doi.org/10.1016/j.ibiod.2023.105569.
33. Babiński L, Izdebska-Mucha D, Waliszewska B. Evaluation of the state of preservation of waterlogged archaeological wood based on its physical properties: basic density vs. wood substance density. J Archaeol Sci. 2014;46:372–83. https://doi.org/10.1016/j.jas.2014.03.038.

34. Humar M, Balzano A, Kržišnik D, Lesar B. Assessment of wooden foundation piles after 125 years of service. Forests. 2021;12(2):143. https://doi.org/10.3390/f12020143.
35. Hemmingson JA, Wong H. Characterization of photochemically degraded newsprint solubles by c-13 nmr and ir spectroscopy. Holzforschung. 1989;43(2):141–7. https://doi.org/10.1515/hfsg.1989.43.2.141.
36. Wozniak M, Kwasniewska-Sip P, Krueger M, Roszyk E, Ratajczak I. Chemical, biological and mechanical characterization of wood treated with propolis extract and silicon compounds. Forests. 2020. https://doi.org/10.3390/f11090907.
37. Li GJ, Peacor DR, Buseck PR, Arkai P. Modification of illite-muscovite crystallite-size distributions by sample preparation for powder xrd analysis. Canad Mineral. 1998;36:1435–51.
38. Onal M, Kahraman S, Sarikaya Y. Differentiation of ␣-cristobalite from opals in bentonites from turkey. Appl Clay Sci. 2007;35(1–2):25–30. https://doi.org/10.1016/j.clay.2006.07.003.
39. Tamilarasi A, Sathish V, Manigandan S, Chandrasekaran A. Data on minerals and crystallinity index of quartz in rock samples collected from paleolithic archaeological site of Attirampakkam, Tamil Nadu. Data Brief. 2021. https://doi.org/10.1016/j.dib.2021.107571.
40. Tang J., Dong F.Q., Dai Q.W., Deng Y.Q., Characterization of atmosphere pm2.5 and Dusffall in Xining (China), Micro-Nano Technology XIV, Pts 1–4 2013; 562–5651422–1427. https://doi.org/10.4028/www.scientific.net/KEM.562-565.1422.
41. Portillo MC, Saiz-Jimenez C, Gonzalez JM. Molecular characterization of total and metabolically active bacterial communities of " white colonizations " in the altamira cave, spain. Res Microbiol. 2009;160(1):41–7. https://doi.org/10.1016/j.resmic.2008.10.002.
42. Bastian F, Alabouvette C, Jurado V, Saiz-Jimenez C. Impact of biocide treatments on the bacterial communities of the lascaux cave. Sci Nat. 2009;96(7):863–8. https://doi.org/10.1007/s00114-009-0540-y.
43. Hoppe B, Krueger D, Kahl T, Arnstadt T, Buscat F, Bauhus J, Wubet T. A pyrosequencing insight into sprawling bacterial diversity and community dynamics in decaying deadwood logs of *Fagus sylvatica* and *Picea abies*. Sci Rep. 2015. https://doi.org/10.1038/srep09456.
44. Rinta-Kanto JM, Sinkko H, Rajala T, Al-Soud WA, Sorensen SJ, Tamminen MV, Timonen S. Natural decay process affects the abundance and community structure of bacteria and archaea in *Picea abies* logs. Fems Microbiol Ecol. 2016. https://doi.org/10.1093/femsec/fiw087.
45. Sun H, Terhonen E, Kasanen R, Asiegbu FO. Diversity and community structure of primary wood-inhabiting bacteria in boreal forest. Geomicrobiol J. 2014;31(4):315–24. https://doi.org/10.1080/01490451.2013.827763.
46. Floudas D, Binder M, Riley R, Barry K, Blanchette RA, Henrissat B, et al. The paleozoic origin of enzymatic lignin decomposition reconstructed from 31 fungal genomes. Science. 2012;336(6089):1715–9. https://doi.org/10.1126/science.1221748.
47. Riley R, Salamov AA, Brown DW, Nagy LG, Floudas D, Held BW, et al. Extensive sampling of basidiomycete genomes demonstrates inadequacy of the white-rot/brown-rot paradigm for wood decay fungi. Proc Natl Acad Sci USA. 2014;111(41):14959. https://doi.org/10.1073/pnas.1418116111.
48. Majaneva M, Rintala J, Blomster J. Taxonomically and functionally distinct ciliophora assemblages inhabiting baltic sea ice. Microb Ecol. 2022;84(4):974–84. https://doi.org/10.1007/s00248-021-01915-4.
49. Duarte S, Baerlocher F, Trabulo J, Cassio F, Pascoal C. Stream-dwelling fungal decomposer communities along a gradient of eutrophication unraveled by 454 pyrosequencing. Fungal Divers. 2015;70(1):127–48. https://doi.org/10.1007/s13225-014-0300-y.
50. Fukasawa Y, Osono T, Takeda H. Dynamics of physicochemical properties and occurrence of fungal fruit bodies during decomposition of coarse woody debris of *Fagus crenata*. J For Res. 2009;14(1):20–9. https://doi.org/10.1007/s10310-008-0098-0.
51. Gessner MO, Swan CM, Dang CK, Mckie BG, Bardgett RD, Wall DH, Haettenschwiler S. Diversity meets decomposition. Trends Ecol Evol. 2010;25(6):372–80. https://doi.org/10.1016/j.tree.2010.01.010.
52. Kodsueb R, Mckenzie EHC, Lumyong S, Hyde KD. Fungal succession on woody litter of *Magnolia liliifera* (magnoliaceae). Fungal Divers. 2008;30:55–72.
53. Nilsson T, Daniel G, Kirk TK, Obst JR. Chemistry and microscopy of wood decay by some higher ascomycetes. Holzforschung. 1989;43(1):11–8. https://doi.org/10.1515/hfsg.1989.43.1.11.
54. Purahong W, Wubet T, Lentendu G, Schloter M, et al. Life in leaf litter: novel insights into community dynamics of bacteria and fungi during litter decomposition. Mol Ecol. 2016;25(16):4059–74. https://doi.org/10.1111/mec.13739.
55. Hallenberg N, Nilsson RH, Antonelli A, Wu S, Maekawa N, Norden B. The peniophorella praetermissa species complex (basidiomycota). Mycol Res. 2007;111:1366–76. https://doi.org/10.1016/j.mycres.2007.10.001.
56. Kale SP, Milde L, Trapp MK, Frisvad JC, Keller NP, Bok JW. Requirement of laea for secondary metabolism and sclerotial production in *Aspergillus flavus*. Fungal Genet Biol. 2008;45(10):1422–9. https://doi.org/10.1016/j.fgb.2008.06.009.
57. Zhu S, Wu H, Wu C, Qiu G, Feng C, Wei C. Structure and function of microbial community involved in a novel full-scale prefix oxic coking wastewater treatment O/H/O system. Water Res. 2019. https://doi.org/10.1016/j.watres.2019.114963.

Publisher's Note